

## **Physical Vapor Deposition of an Oriented Metal–Organic Framework**

### **HKUST-1 Thin Film on an Insulating Substrate**

Shunta Iwamoto<sup>1</sup>, Ryo Nakayama<sup>2</sup>, Seungmin Chon<sup>1</sup>, Ryota Shimizu<sup>2</sup>, and Taro Hitosugi<sup>1,2</sup>

<sup>1</sup> School of Materials and Chemical Technology, Tokyo Institute of Technology, Tokyo 152-8552, Japan

<sup>2</sup> Department of Chemistry, The University of Tokyo, Tokyo 113-0033, Japan

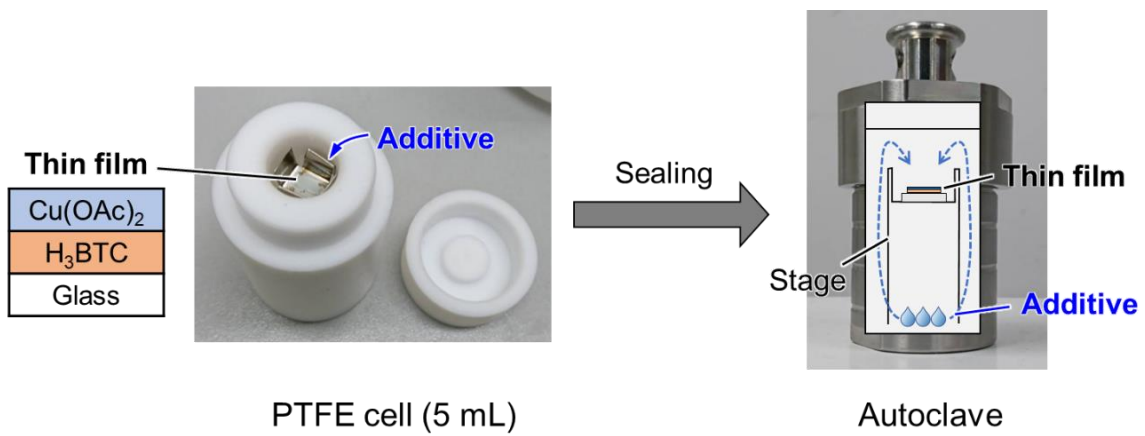


Fig. S1. Setup for the annealing of thin films with solvent vapor.

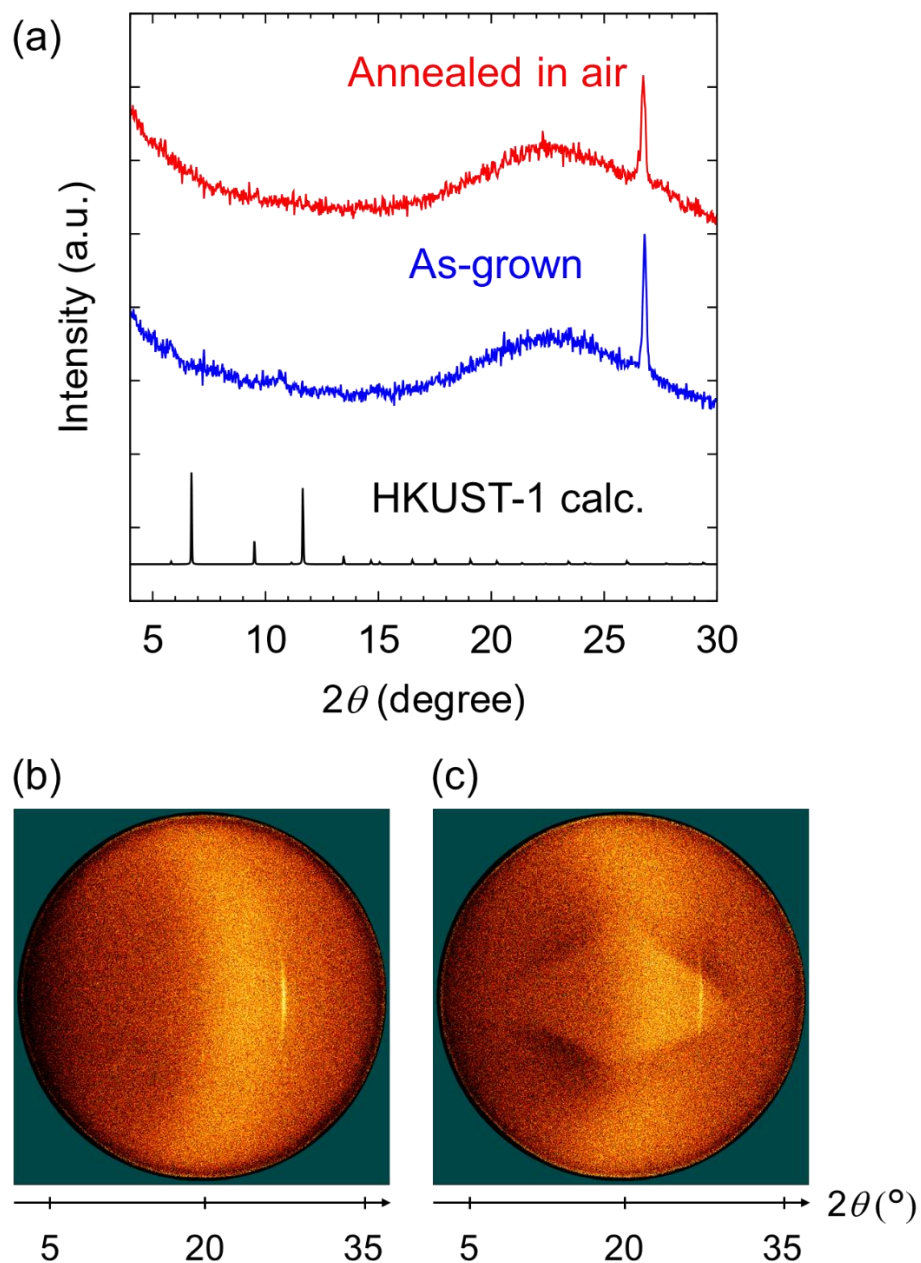


Fig. S2. (a) Out-of-plane X-ray diffraction patterns of the as-grown thin film and thin film annealed in air. Two-dimensional X-ray diffraction patterns of the (b) as-grown thin film and (c) thin film annealed in air.

Figure S2(a) shows the out-of-plane XRD patterns of the as-grown and annealed-in-air films. The XRD patterns do not show the diffraction peaks of HKUST-1. The peak at  $2\theta$

=  $26.8^\circ$  observed for both films does not correspond with the precursors or HKUST-1 powder. The spot-like diffraction at  $2\theta = 26.8^\circ$  indicates that the unidentified product is oriented out-of-plane (Figs. S2(b) and (c)). The peak at  $2\theta = 26.8^\circ$  will be identified in future work because it disappears after annealing with solvent vapor.

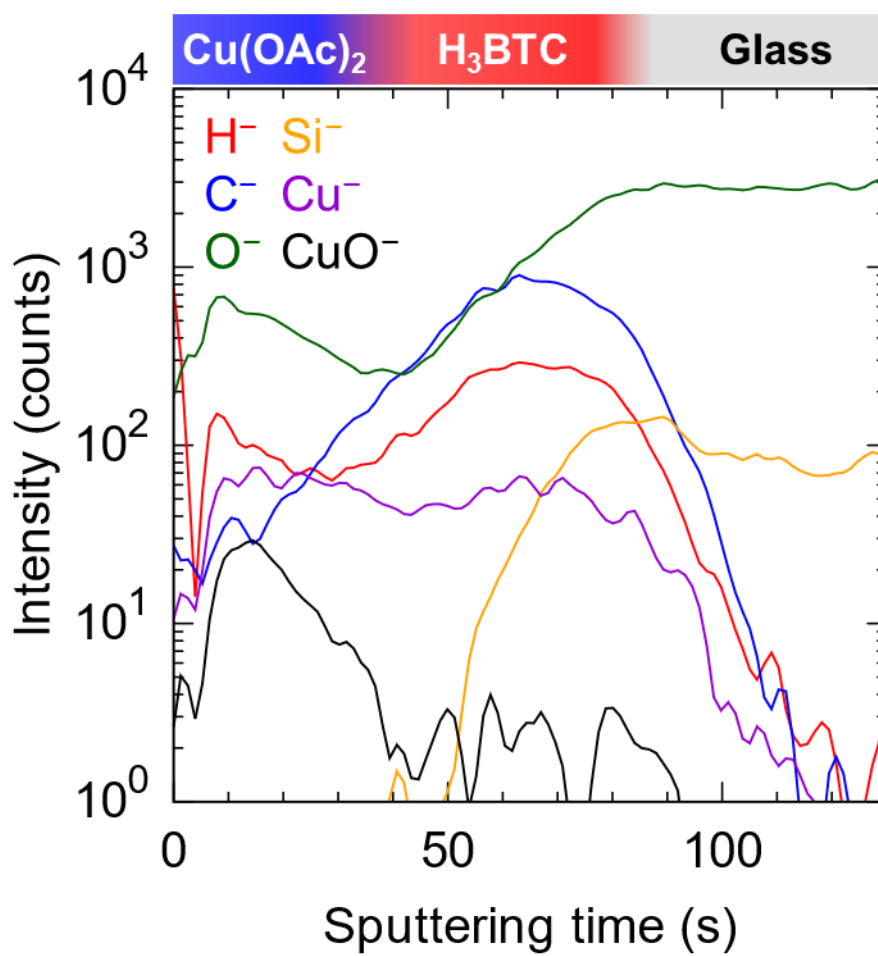


Fig. S3. Depth profiles of the chemical components of the as-grown thin film obtained by secondary ion mass spectroscopy.

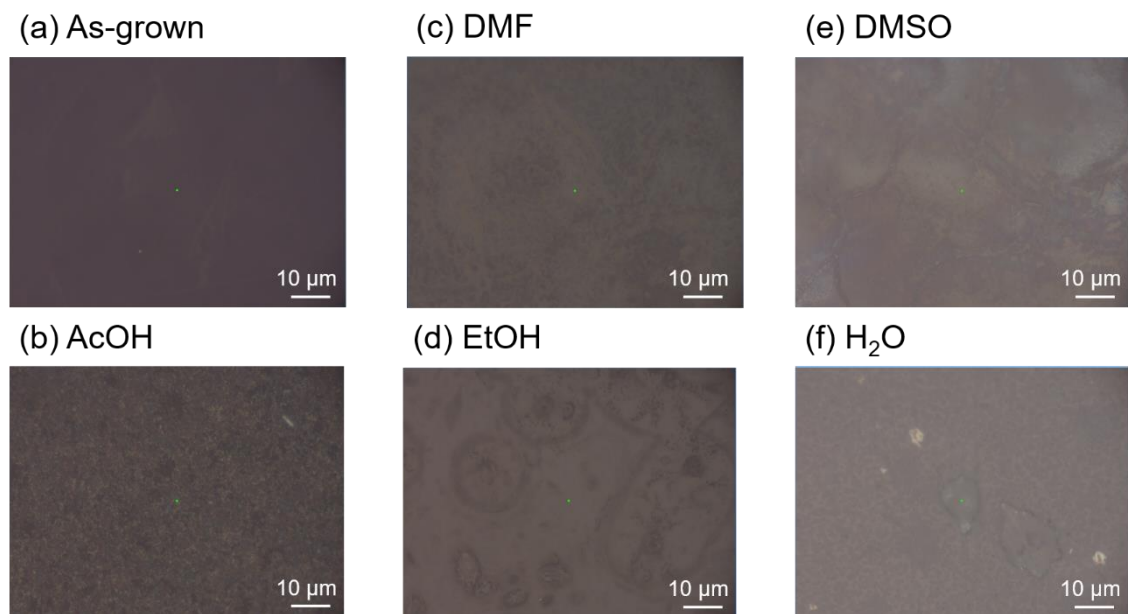


Fig. S4 Optical microscopy image of the thin films of (a) As-grown (before annealing) and annealed with (b) acetic acid (AcOH), (c) *N,N*-dimethylformamide (DMF), (d) ethanol (EtOH), (e) dimethyl sulfoxide (DMSO), and (f) water (H<sub>2</sub>O)

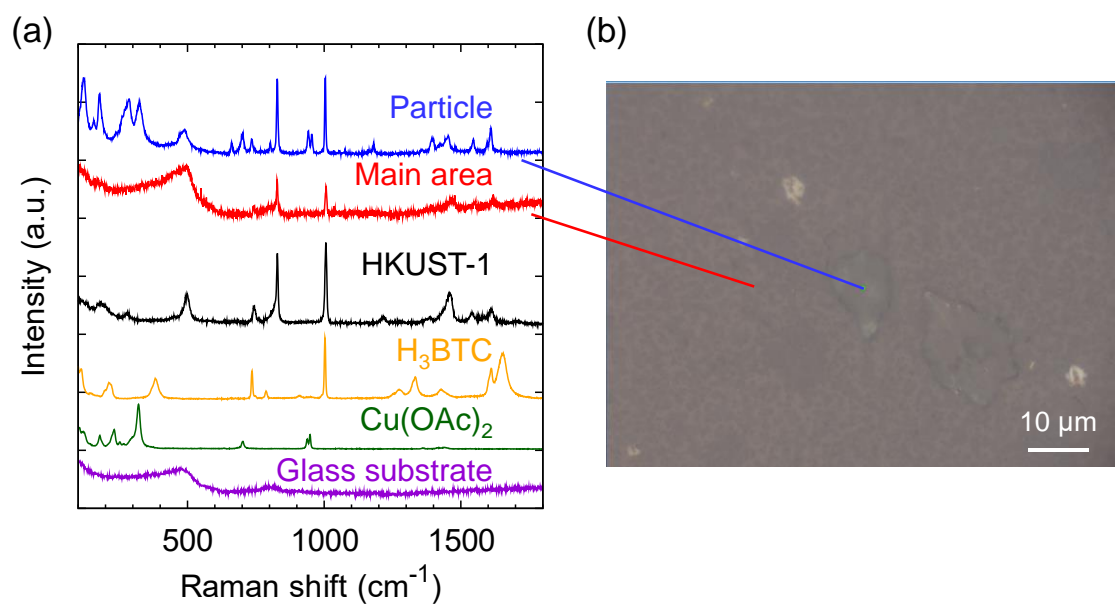


Fig. S5 (a) Raman spectra and (b) optical microscopy image of the film annealed with water vapor

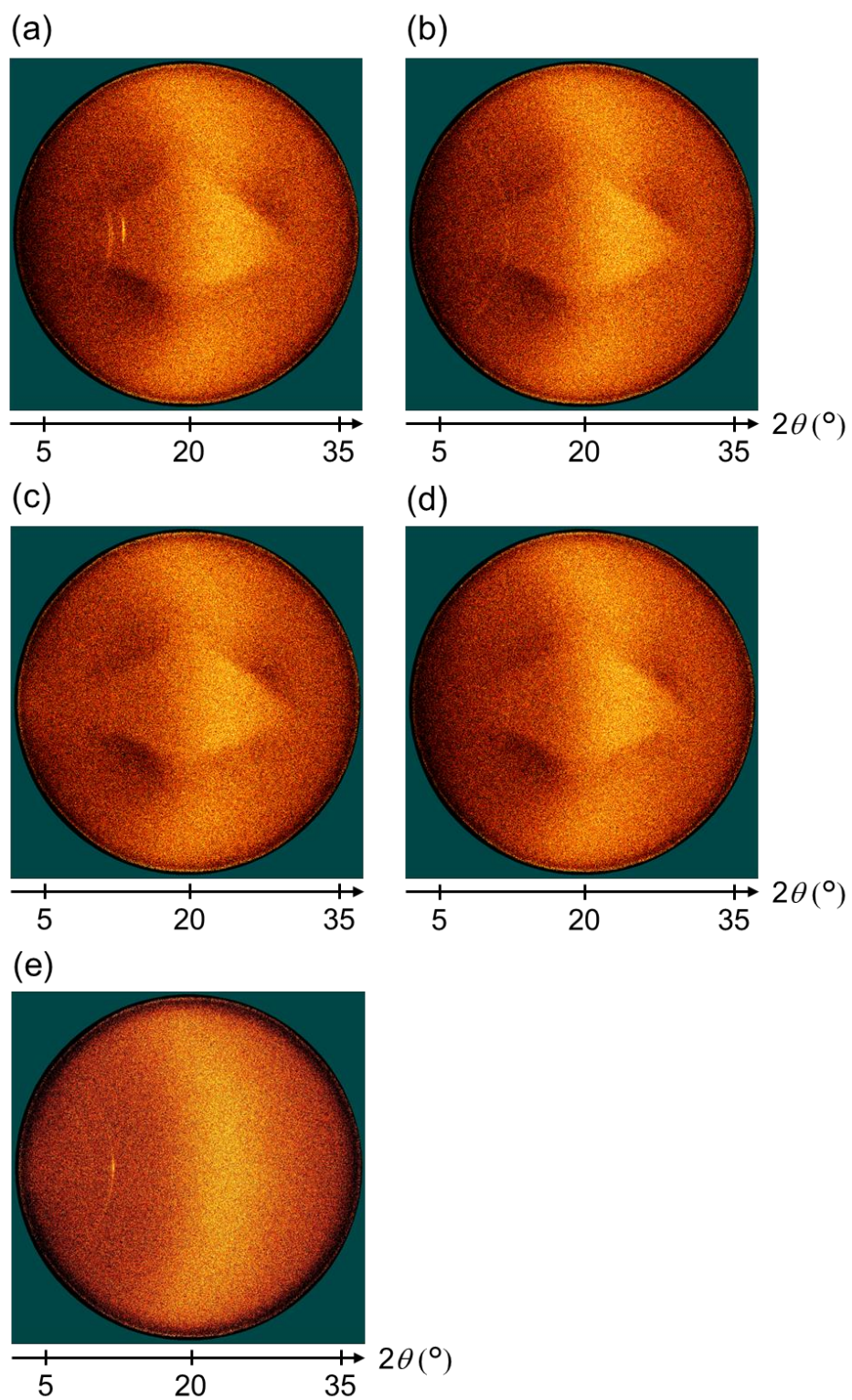


Fig. S6. Two-dimensional X-ray diffraction patterns of (a) water, (b) dimethyl sulfoxide, (c) *N,N*-dimethylformamide, (d) ethanol, and (e) acetic acid.

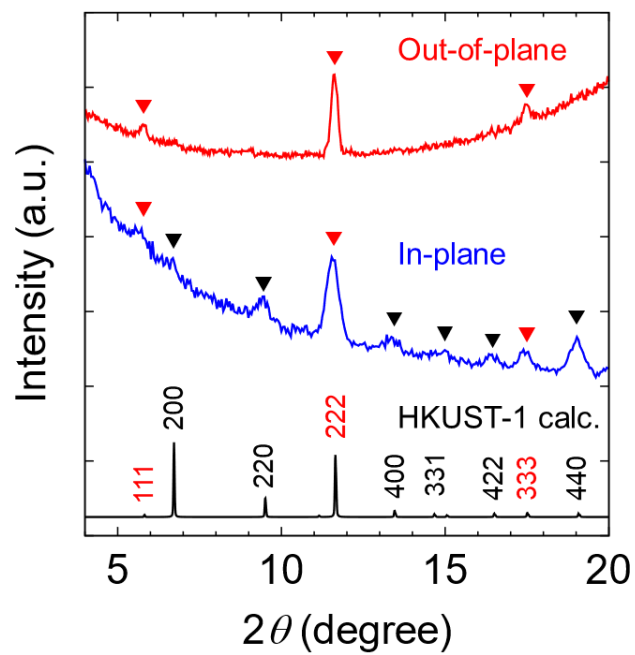


Fig. S7. Out-of-plane and in-plane XRD patterns of HKUST-1 thin film

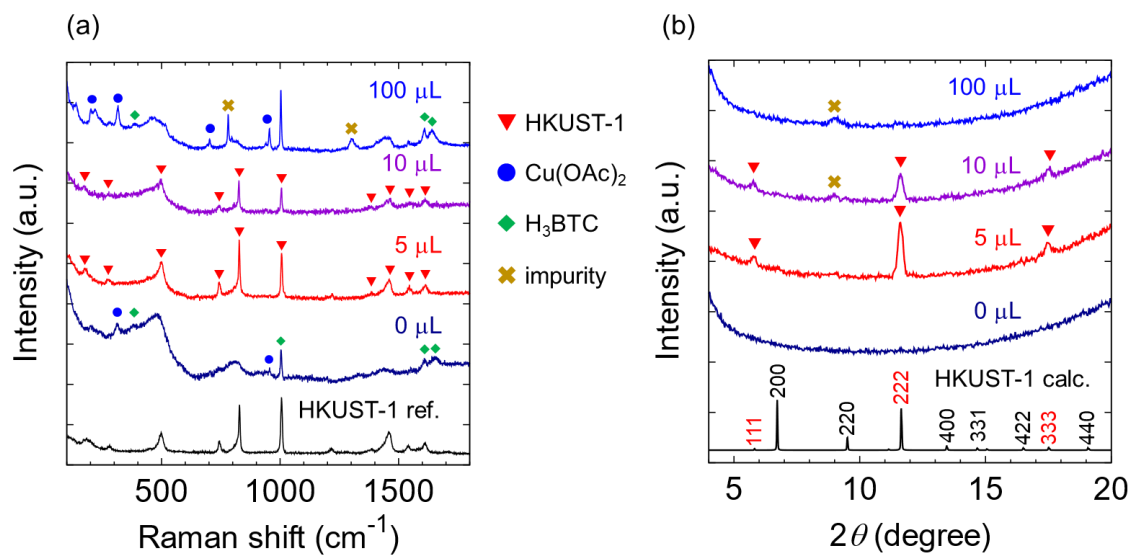


Fig. S8. (a) Raman spectra and (b) out-of-plane X-ray diffraction patterns of films annealed using different volumes of acetic acid.

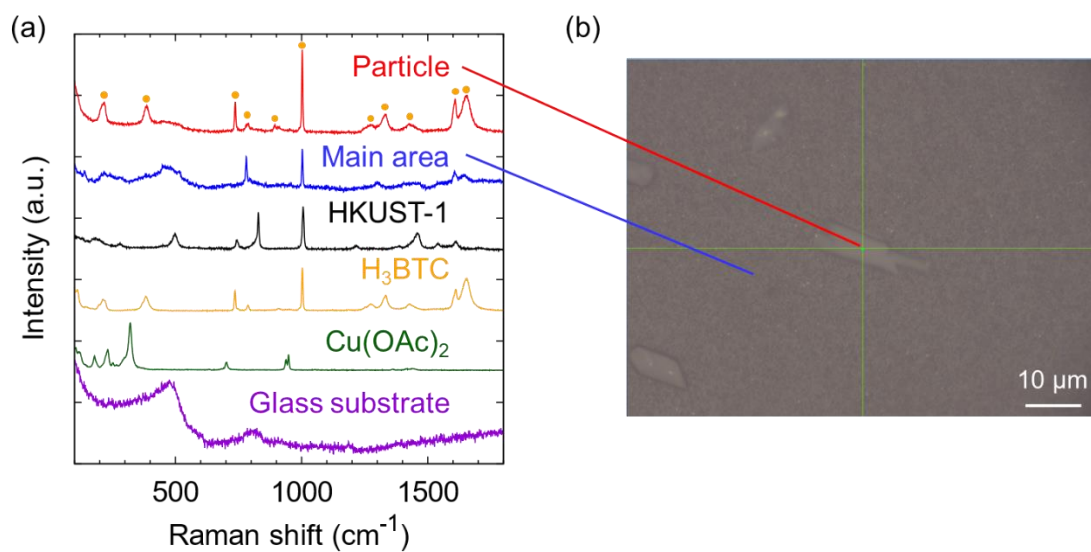


Fig. S9. (a) Raman spectra and (b) optical microscopy image of the film synthesized using a Cu:1,3,5-benzenetricarboxylate (BTC) stoichiometric ratio of 2:2.

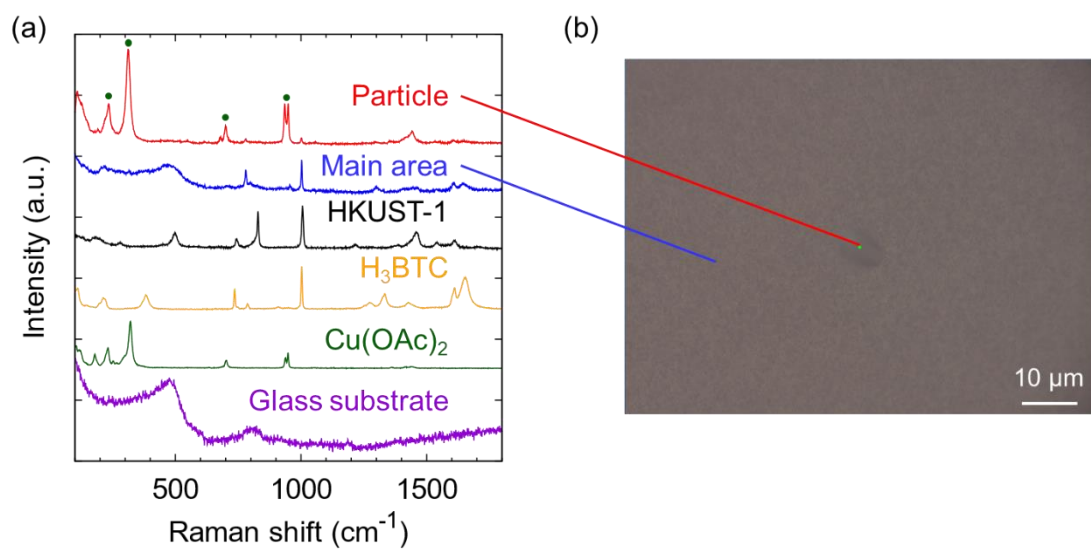


Fig. S10. (a) Raman spectra and (b) optical microscopy image of the film synthesized using a Cu:1,3,5-benzenetricarboxylate (BTC) stoichiometric ratio of 4:2.

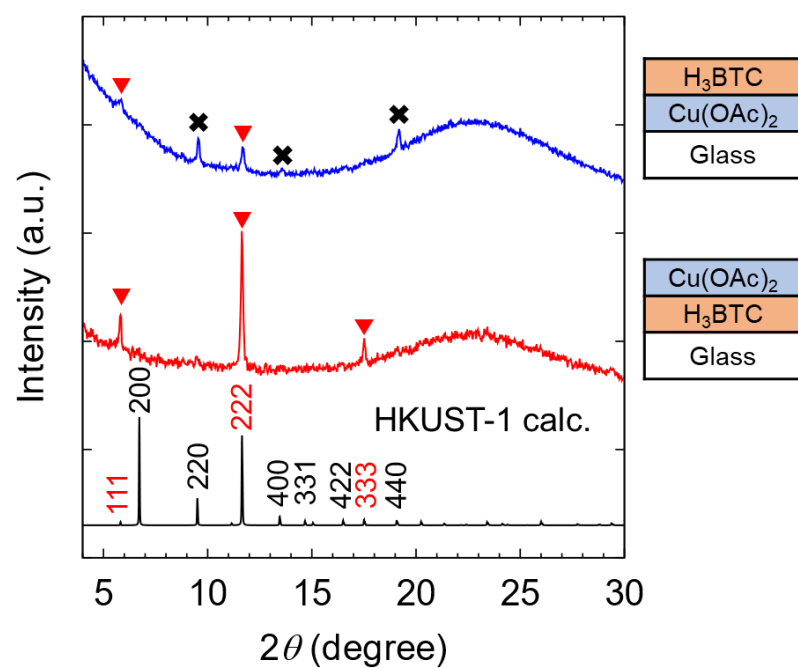


Fig. S11. out-of-plane X-ray diffraction pattern of thin films with different deposition sequence.

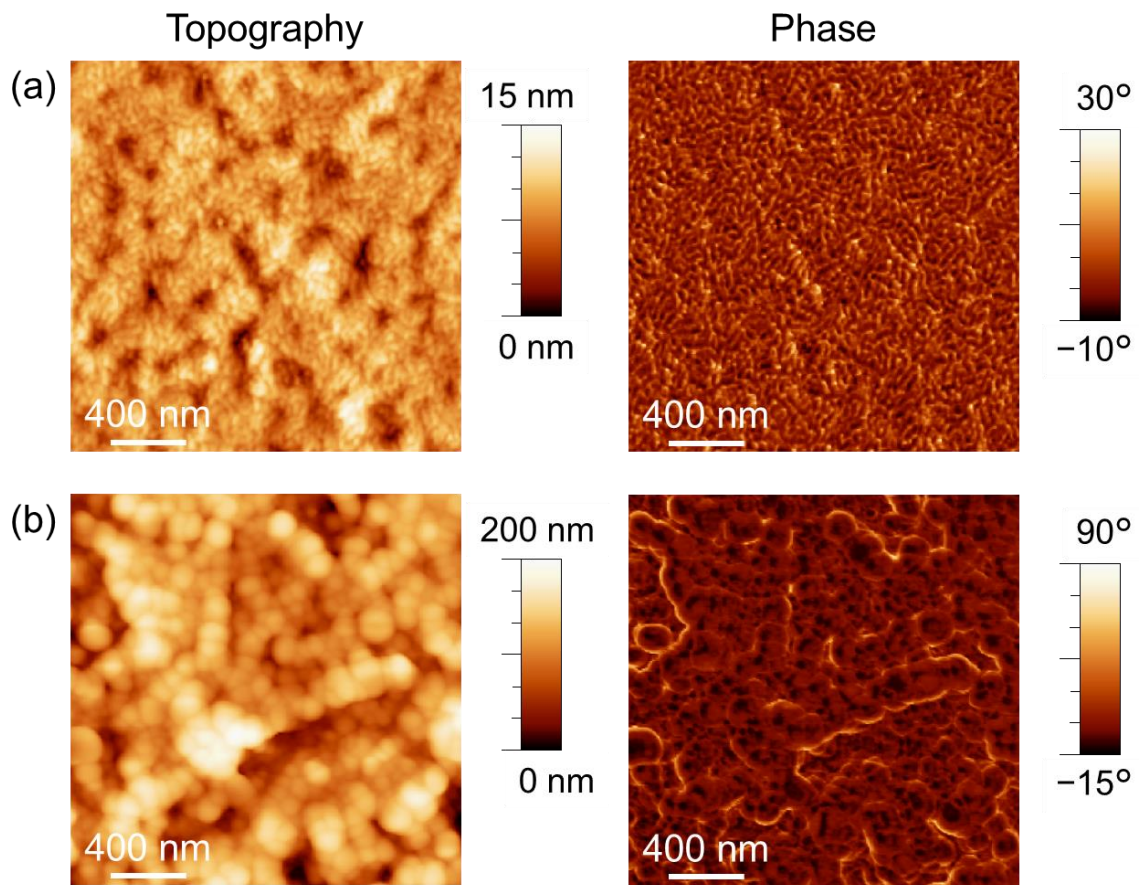


Fig. S12. Atomic force microscopy images of the (a) as-grown and (b) (111)-oriented HKUST-1 films.

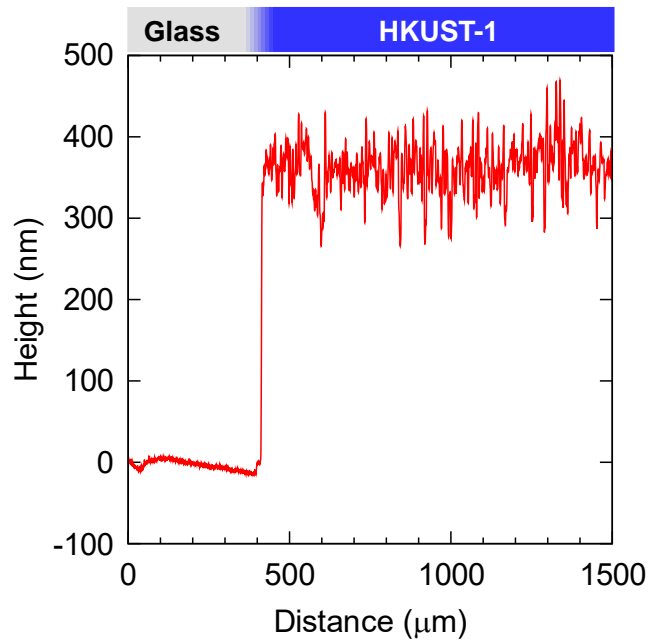


Fig. S13. Surface profile of (111)-oriented HKUST-1 thin film

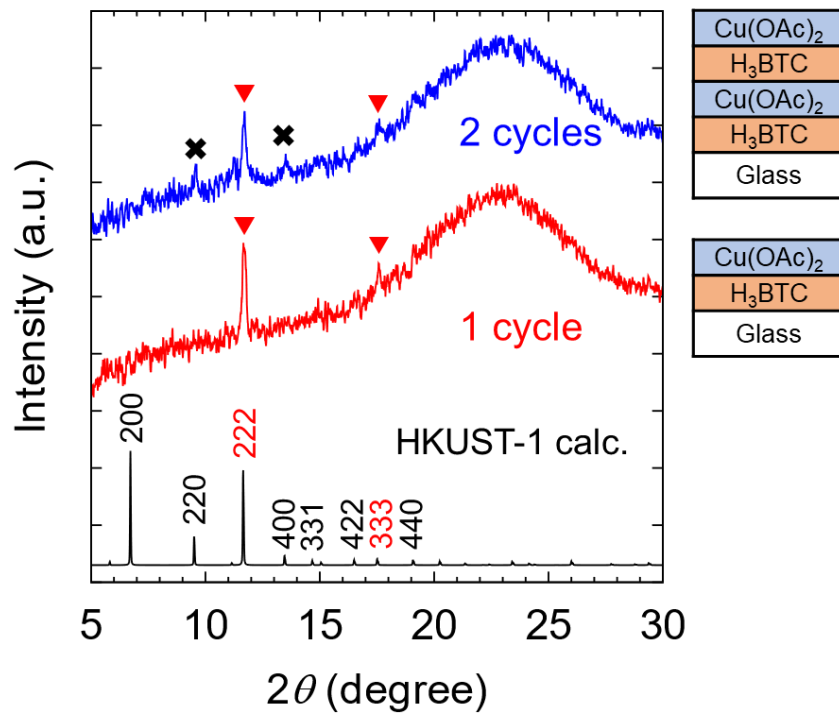


Fig. S14. out-of-plane X-ray diffraction pattern of thin films with different deposition sequence.

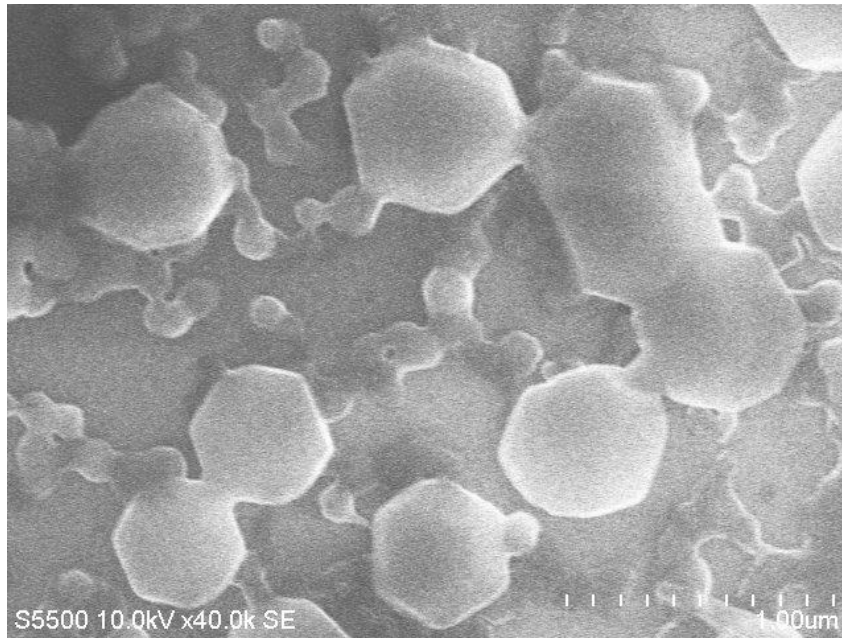


Fig. S15. Enlarged SEM image of (111)-oriented HKUST-1 thin film

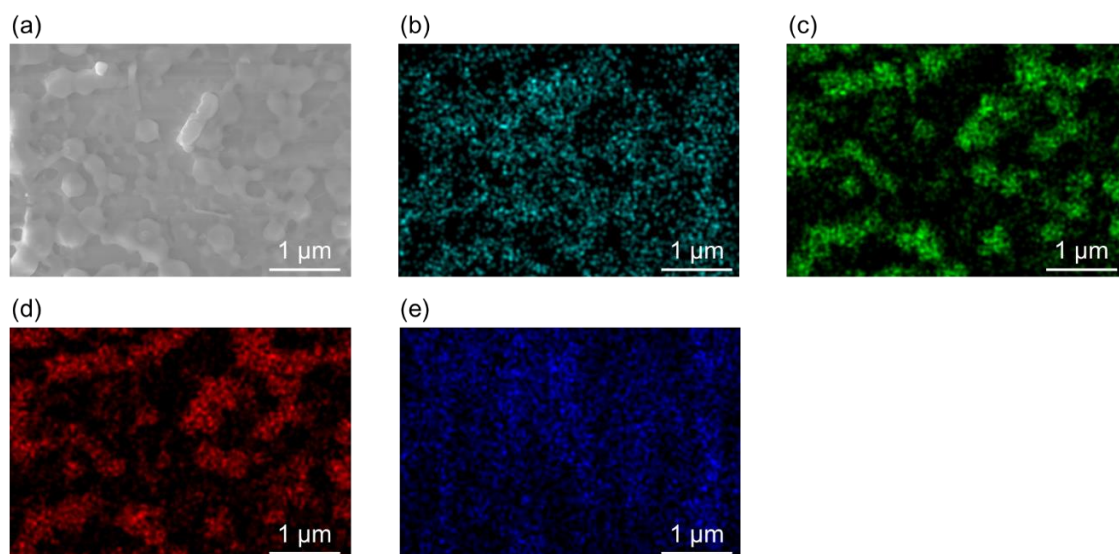


Fig. S16. (a) Scanning electron microscopy image and energy-dispersive X-ray spectroscopy mapping of (b) Si, (c) C, (d) Cu, and (e) O in the (111)-oriented HKUST-1 film.

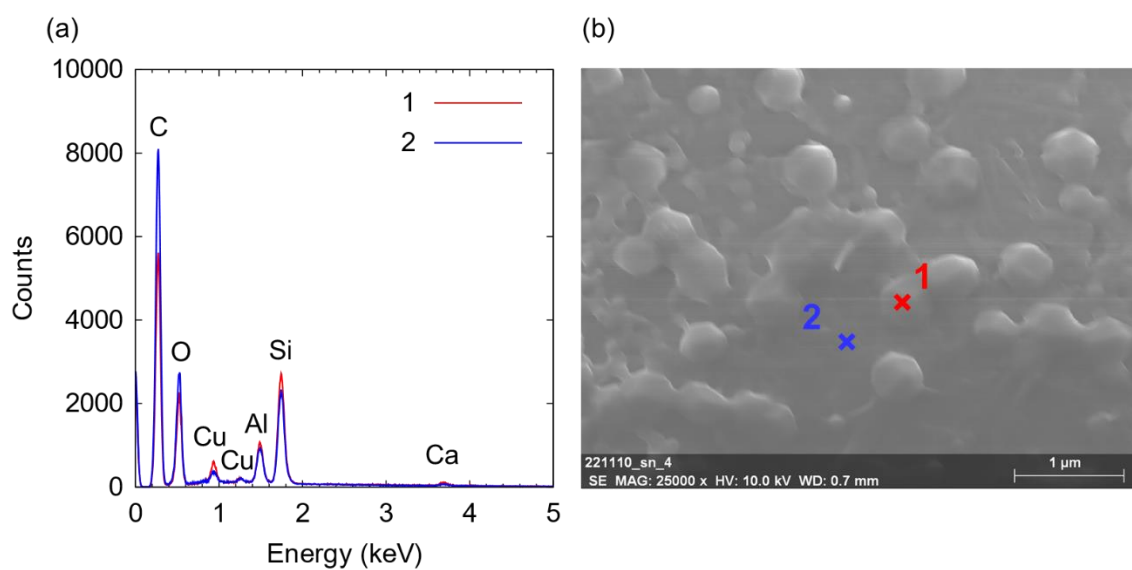


Fig. S17. (a) Point analysis of the energy-dispersive X-ray spectroscopy spectra and (b) corresponding sampling points in the scanning electron microscopy image of the (111)-oriented HKUST-1 film.

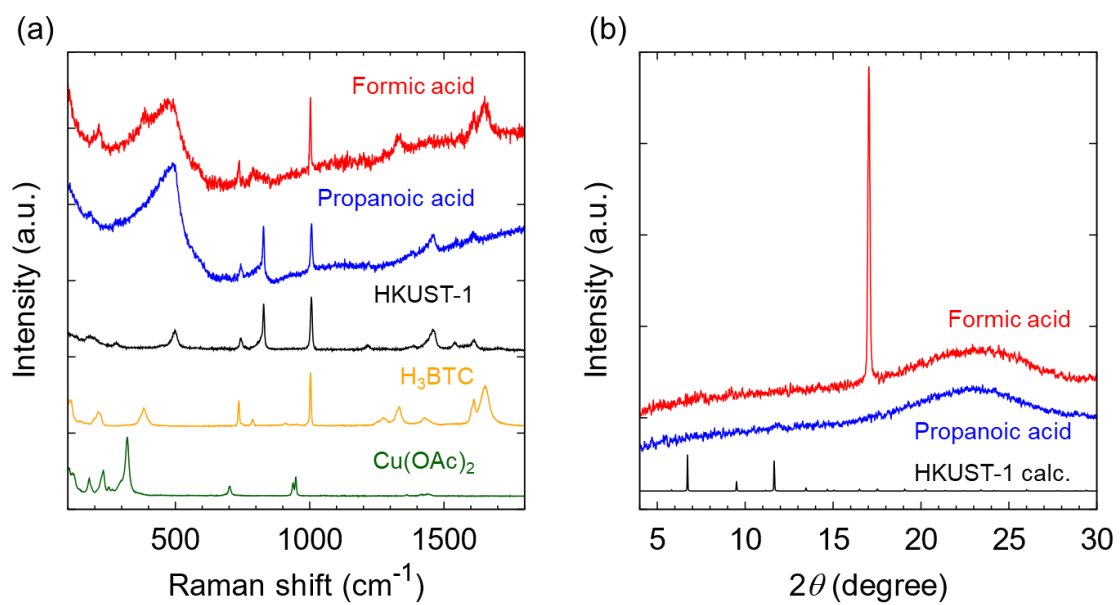


Fig. S18. (a) Raman spectra and (b) X-ray diffraction patterns of films annealed with different monocarboxylic acids.

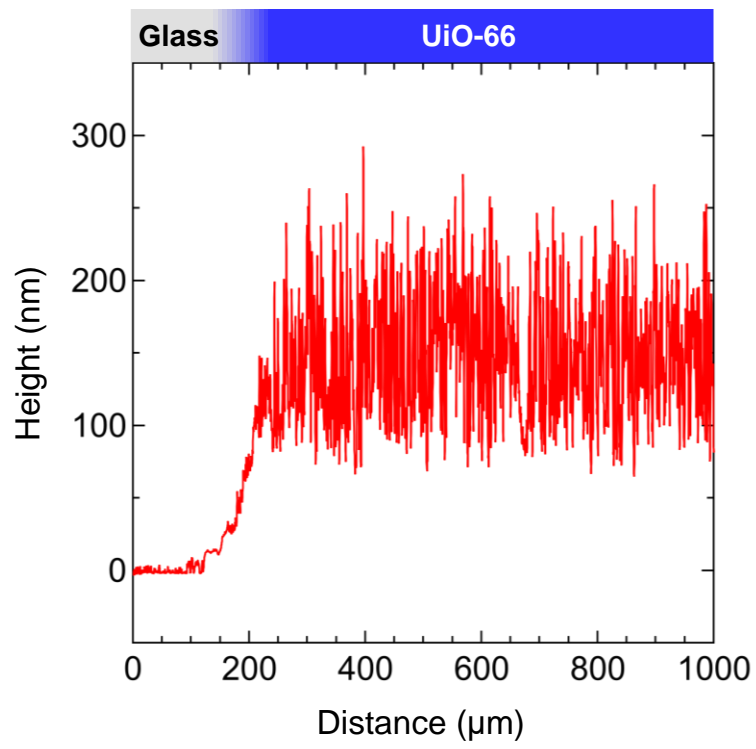


Fig. S19. Surface profile of UiO-66 thin film on a glass substrate